Rab10 and myosin-Va mediate insulin-stimulated GLUT4 storage vesicle translocation in adipocytes

Yu Chen,[2] Yan Wang,[1] Jinzhong Zhang,[1] Yongqiang Deng,[1] Li Jiang,[1] Eli Song,[1] Xufeng S. Wu,[3] John A. Hammer,[3] Tao Xu,[1] and Jennifer Lippincott-Schwartz[2]

[1]Institute of Biophysics, Chinese Academy of Sciences, Beijing 100101, China
[2]Cell Biology and Metabolism Program, Eugene Kennedy Shriver National Institute of Child Health and Human Development; and [3]Laboratory of Cell Biology, National Heart, Lung, and Blood Institute, National Institutes of Health, Bethesda, MD 20892

Rab proteins are important regulators of insulin-stimulated GLUT4 translocation to the plasma membrane (PM), but the precise steps in GLUT4 trafficking modulated by particular Rab proteins remain unclear. Here, we systematically investigate the involvement of Rab proteins in GLUT4 trafficking, focusing on Rab proteins directly mediating GLUT4 storage vesicle (GSV) delivery to the PM. Using dual-color total internal reflection fluorescence (TIRF) microscopy and an insulin-responsive aminopeptidase (IRAP)-pHluorin fusion assay, we demonstrated that Rab10 directly facilitated GSV translocation to and docking at the PM. Rab14 mediated GLUT4 delivery to the PM via endosomal compartments containing transferrin receptor (TfR), whereas Rab4A, Rab4B, and Rab8A recycled GLUT4 through the endosomal system. Myosin-Va associated with GSVs by interacting with Rab10, positioning peripherally recruited GSVs for ultimate fusion. Thus, multiple Rab proteins regulate the trafficking of GLUT4, with Rab10 coordinating with myosin-Va to mediate the final steps of insulin-stimulated GSV translocation to the PM.

Introduction

Insulin stimulates glucose uptake into adipocytes and muscle tissues by recruiting GLUT4 to the plasma membrane (PM). The exocytosis of GLUT4 in response to insulin is achieved through physical trafficking of storage vesicles enriched in GLUT4 called GLUT4 storage vesicles (GSVs) from intracellular sites to the PM (Bryant et al., 2002; Watson et al., 2004; Foley et al., 2011). A signaling cascade involving PI3K, AKT/PKB, AS160, and Rab proteins regulates such trafficking. In this cascade, PI3K and AKT/PKB are activated in response to insulin, causing phosphorylation of the RabGAP protein AS160 by AKT (Kane et al., 2002; Sano et al., 2003; Sano et al., 2011). When nonphosphorylated, AS160 retains GLUT4 within the cell by inactivating cognate Rab proteins involved in GLUT4 vesicle delivery to the PM (Sano et al., 2003; Eguez et al., 2005; Larance et al., 2005). When phosphorylated in response to insulin stimulation, AS160 loses its GAP activity. The cognate Rab proteins now become active, causing GLUT4 translocation to the PM (Sakamoto and Holman, 2008; Foley et al., 2011). Consequently, PM levels of GLUT4 increase when cognate Rabs are activated by AS160 knockdown (Eguez et al., 2005; Larance et al., 2005), and decrease when cognate Rabs are inactive with overexpression of AS160-4P, a constitutively active form of AS160 (Sano et al., 2003).

GLUT4 follows a complex intracellular trafficking pathway, passing through early and recycling endosomes before being resorted into GSVs (Bryant et al., 2002; Foley et al., 2011). This results in a variety of different Rab proteins being associated with GLUT4-containing compartments. Indeed, membrane fractionation and immunopurification studies have revealed that Rab2A (Mîinea et al., 2005), Rab4 (Cormont et al., 1993), Rab8 (Mîinea et al., 2005), Rab10 (Larance et al., 2005), Rab11 (Larance et al., 2005), and Rab14 (Larance et al., 2005; Mîinea et al., 2005) all associate with GLUT4-containing compartments.

Y. Chen, Y. Wang, and J. Zhang contributed equally to this paper.

Correspondence to Jennifer Lippincott-Schwartz: lippincj@mail.nih.gov; or Tao Xu: xutao@ibp.ac.cn

Y. Wang's present address is Howard Hughes Medical Institute, University of Texas Southwestern Medical Center, Dallas, TX 75390.

Abbreviations used in this paper: GSV, GLUT4 storage vesicle; IRAP, insulin-responsive aminopeptidase; PM, plasma membrane; TfR, transferrin receptor; TIRF, total internal reflection fluorescence.

The Rockefeller University Press $30.00
J. Cell Biol. Vol. 198 No. 4 545–560
www.jcb.org/cgi/doi/10.1083/jcb.201111091

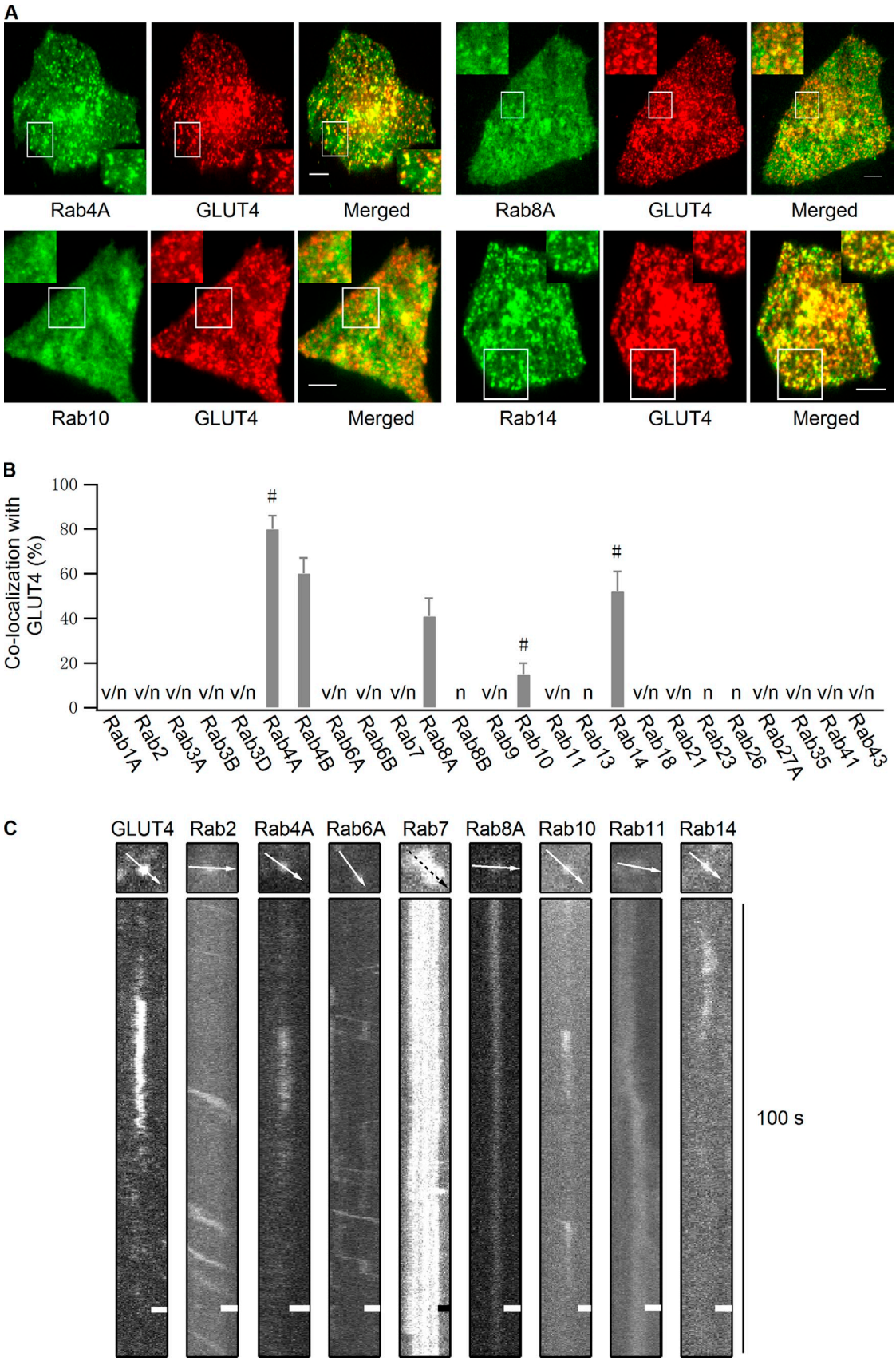

Figure 1. **Multiple Rab proteins reside on GLUT4 vesicles.** (A) Rab proteins tagged with EGFP and GLUT4-mCherry were cotransfected into adipocytes, and their colocalization was examined in the absence of insulin stimulation using dual-color TIRF microscopy. Bars, 4 µm. (B) Quantification of Rab protein colocalization with GLUT4 vesicles in the absence of insulin stimulation. All Rab proteins were tagged with mKO and quantified for their colocalization with GLUT4-EGFP vesicles. Rab4A, Rab4B, Rab8A, Rab10, and Rab14, which showed overlap with GLUT4-EGFP vesicles, were then tagged with EGFP

A major challenge in the GLUT4 trafficking field has been determining what Rab proteins regulate which steps in GLUT4 delivery to the PM in response to insulin. Researchers have used numerous strategies to address this question. One approach measured the response by different Rab proteins to AS160 GAP activity. Although some candidate Rab proteins were identified, because AS160 GAP activity is likely to be promiscuous toward multiple Rab proteins, no decisive conclusion could be drawn regarding the specific role of any of the Rab proteins in GLUT4 trafficking (Mîinea et al., 2005). Another method monitored insulin-stimulated GTP loading of Rab proteins, identifying Rab8A and Rab13 as important factors for GLUT4 translocation in muscle cells (Sun et al., 2010). Using similar techniques in adipocytes, however, did not detect GTP loading of the candidate Rab protein (Sano et al., 2008). An additional approach, pointing to Rab10, examined how inhibiting particular Rabs affected PM delivery of GLUT4 in response to insulin stimulation (Sano et al., 2007, 2008). Conclusions from this approach are complicated by potential mistargeting of GLUT4 before insulin stimulation because GLUT4 traffics through many different endocytic compartments. It has thus remained unclear what Rab proteins are involved in GLUT4 translocation to the PM and which are involved in other steps of GLUT4 trafficking.

Given the existence of multiple routes for GLUT4 trafficking within the cell, with different Rab proteins possibly associating with GLUT4 as it traffics through different compartments, we reasoned that a direct imaging approach of Rab proteins and their involvement in GLUT4 delivery to the PM would prove valuable. Here, we used advanced imaging techniques to identify and characterize Rab proteins involved in GSV delivery to the PM during insulin stimulation in adipocytes. Monitoring GSV translocation in real time in live cells using the pH-sensitive fluorescence protein pHluorin and dual-color total internal reflection fluorescence (TIRF) microscopy, we screened a library of different Rab proteins for colocalization with GSVs or other GLUT4 compartments, studying their prefusion and postfusion behaviors and the role of myosin motors. Our data suggest that Rab10 activation on GSVs underlies insulin-stimulated GSV recruitment to the PM, with Rab14, Rab4A, Rab4B, and Rab8A involved in other steps in GLUT4 trafficking. Activated Rab10 on the peripherally recruited GSV then coordinates with myosin-Va to prepare the vesicle for final fusion.

Results

Diverse Rab proteins reside on GLUT4-containing compartments close to the PM

We began by visually screening the intracellular distribution of 25 candidate Rab proteins known to traffic through endosomal pathways (Schwartz et al., 2007; Stenmark, 2009). Using TIRF microscopy to restrict the field of view to only ∼90 nm from the PM, we tested whether any of these Rab proteins overlapped with GLUT4 vesicles close to the PM. Several Rab proteins had steady-state pools on GLUT4 vesicles close to the PM. Among these, Rab4A, Rab4B, Rab14, and Rab8A showed the highest frequency of colocalization with GLUT4 vesicles, and Rab10 showed a lower colocalization frequency (Fig. 1, A and B). Other Rab proteins either showed no colocalization with GLUT4 vesicles or did not localize close to the PM (Fig. 1 B, Fig. S1, and Table S1).

We next examined the behavior of vesicles marked by the different Rab proteins under insulin stimulation by TIRF microscopy (Fig. 1 C). Individual Rab proteins were tagged with the fluorescent protein mKO to visualize the dynamics of the vesicles they labeled. Upon entering the TIRF zone at a steep angle, insulin-responsive GLUT4 vesicles usually dock at the PM for a short period before undocking or fusing with the PM (Lizunov et al., 2005; Bai et al., 2007; Huang et al., 2007). In our image sequences, insulin-responsive GLUT4-EGFP vesicles near the PM exhibited this behavior (Fig. 1 C, GLUT4), as did vesicles containing mKO-labeled Rab4A, Rab10, or Rab14 (Fig. 1 C). The docking behavior displayed by these vesicles under insulin stimulation included a sudden appearance in the TIRF zone and then docking at the PM. This was followed by the disappearance of the vesicle, likely representing the vesicle undocking or fusing with the PM. Vesicles associated with other Rab proteins either stayed predominantly immobile (exemplified by Rab7-, Rab8A-, and Rab11-containing vesicles) or often moved laterally (exemplified by Rab2- and Rab6A-containing vesicles) beneath the PM (Fig. 1 C). These data suggest that although many different Rab proteins associate with GLUT4 compartments close to the PM, Rab4A, Rab10, and Rab14 most likely associate with GLUT4 vesicles undergoing docking and fusion in response to insulin stimulation.

Selective visualization of insulin-responsive GLUT4 vesicles using insulin-responsive aminopeptidase (IRAP)-pHluorin

To further identify the Rab proteins involved in PM delivery of GLUT4, we used the GLUT4 vesicle fusion probe, IRAP tagged with pHluorin (IRAP-pHluorin). The IRAP portion of this probe contains the cytoplasmic and transmembrane region of full-length IRAP, ensuring that the membrane targeting of this probe is identical to full-length IRAP (Jiang et al., 2008). The pHluorin (Miesenböck et al., 1998) portion of the probe produces a fluorescence signal in response to a shift from low to high pH. These characteristics enable the IRAP-pHluorin probe to target to GLUT4-containing acidic vesicles, similar

and further tested with GLUT4-mCherry. Switching fluorescent protein tags in this manner had no significant effect on the extent of colocalization. v/n, Rab vesicles were observed close to the PM but had no colocalization with GLUT4; n, no Rab vesicle were observed close to the PM; #, Rab proteins that showed frequent docking behavior after insulin stimulation. Data are represented as mean ± SEM (error bars). The number of cells and GLUT4 vesicles analyzed is as follows: Rab4A, *n* = 3 cells and 144 vesicles; Rab4B, *n* = 3 cells and 137 vesicles; Rab8A, *n* = 3 cells and 153 vesicles; Rab10, *n* = 3 cells and 190 vesicles; and Rab14, *n* = 3 cells and 140 vesicles. See also Table S1 and Fig. S1. (C) mKO-tagged Rab proteins were transfected into adipocytes, and 3 min after insulin stimulation their movement beneath the PM was compared with insulin-responsive GLUT4-EGFP vesicle docking processes using TIRF microscopy. Bars, 0.64 µm.

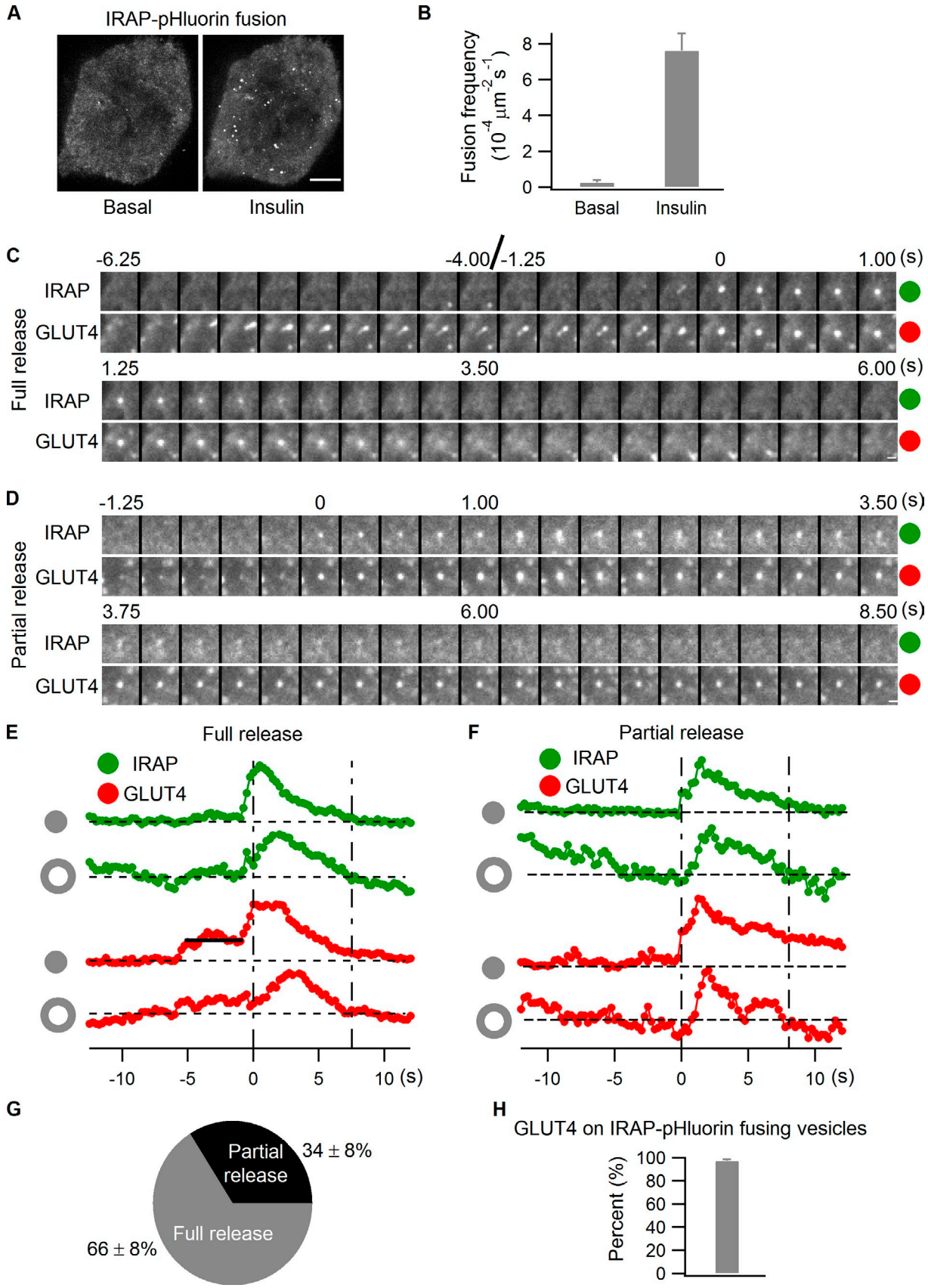

Figure 2. **Full versus partial release of IRAP-pHluorin vesicles at the PM.** (A and B) IRAP-pHluorin was transfected into adipocytes. Vesicle fusions at the PM were captured using TIRF microscopy 3 min after insulin stimulation, and fusion rates were quantified. Adipocytes showing no vesicle fusion before insulin stimulation were preferentially chosen, as they usually responded to insulin very well, producing many fusion events after stimulation. (A) The maximum projections of the subtraction image stacks of two videos acquired from the same cell before and 3 min after insulin stimulation. The subtraction image

to full-length IRAP (Kandror and Pilch, 1994; Ross et al., 1996), and to produce a fluorescence signal in response to pH change when the acidic lumen of the vesicle mixes with the neutral external environment upon opening of the fusion pore (Jiang et al., 2008).

To demonstrate that IRAP-pHluorin can highlight fusion of GLUT4 vesicles at the PM in this fashion, we transfected IRAP-pHluorin into adipocytes and then monitored vesicle fusion events by TIRF microscopy. We found that insulin treatment stimulated numerous vesicle fusions detectable by IRAP-pHluorin fluorescence at the PM in adipocytes (Fig. 2, A and B). IRAP-pHluorin was then coexpressed with GLUT4-mCherry in adipocytes, and fusion events observed after insulin stimulation were examined to confirm that the fusing vesicles contained both GLUT4 and IRAP. To monitor fusion, we tracked the intensities of GLUT4-mCherry and IRAP-pHluorin at the fusion site by dual-color TIRF microscopy (Fig. 2, C–F). Two types of fusion events were observed, including full and partial releases. In the full release event shown in Fig. 2 (C and E), the fusing vesicle was first apparent in the GLUT4-mCherry channel, followed by a transient rise in the IRAP-pHluorin signal corresponding to fusion of the vesicle. After fusion, IRAP and GLUT4 completely diffused away from the fusion site (Fig. 2, C and E). In the partial release event shown in Fig. 2 (D and F), only a small portion of GLUT4 and IRAP were released from the vesicle before the fusion pore closed again. Afterward, the vesicle continued to stay at the fusion site, with GLUT4-mCherry intensity persisting over time while IRAP-pHluorin intensity already dropped back to the background level because of the vesicular lumen reacidification (Fig. 2, D and F). Quantifying the frequency of full and partial release events after insulin stimulation reveals that full release dominated the fusion of IRAP-pHluorin vesicles (Fig. 2 G and Video 1), as described previously (Jiang et al., 2008; Xu et al., 2011). As for the presence of GLUT4-mCherry on insulin-stimulated IRAP-pHluorin fusing vesicles, >95% of fusing vesicles had GLUT4 associated with them (Fig. 2 H), which indicates that virtually all exocytosing IRAP-pHluorin vesicles are GLUT4-containing compartments. Together, these results defined the variety and characteristics of IRAP-pHluorin fusion events in our imaging assays.

A proportion of insulin-responsive GLUT4 vesicles in adipocytes represent recycling endosomes

GLUT4 and IRAP circulate constitutively through the endocytic pathway in addition to localizing to GSVs. In this process, they undergo periodic exocytosis with other endocytic membrane components, such as transferrin receptor (TfR; Bryant et al., 2002; Maxfield and McGraw, 2004). Therefore, a fraction of GLUT4/IRAP exocytotic events detected using IRAP-pHluorin may result from recycling endosomal compartments rather than GSVs. To address this possibility and to quantify its extent, we cotransfected cells with IRAP-pHluorin and TfR-mCherry to see if any of the fusing vesicles contained TfR-mCherry. To ensure we could detect such events, we first coexpressed IRAP-pHluorin and TfR-mCherry in 3T3-L1 fibroblast cells, which are pre-adipocytes without GSV (Fig. S2; Zeigerer et al., 2002). Most IRAP-pHluorin vesicles undergoing PM fusion after insulin stimulation in these cells contained TfR (Fig. 3, A, C, and E; and Video 2), which is consistent with the localization of GLUT4 on TfR-positive endosomes in these cells (Fig. S2). In 3T3-L1 fibroblast cells, therefore, IRAP-pHluorin vesicles that fuse at the PM after insulin stimulation represent endocytic compartments containing TfR.

We next examined PM translocation and fusion events of vesicles containing IRAP-pHluorin and TfR-mCherry in differentiated adipocytes. These cells had a large population of GLUT4 vesicles with no TfR (Fig. S2; Zeigerer et al., 2002). Unlike in 3T3-L1 fibroblast cells, only a small portion (<35%) of IRAP-pHluorin vesicles that fused with the PM in response to insulin stimulation had TfR in adipocytes (Fig. 3, B, D, and E; and Video 3). This suggests that in adipocytes the bulk of insulin-stimulated exocytosing IRAP-pHluorin vesicles are bona fide GSVs. There is only a small pool of endosomal compartments containing both GLUT4 and TfR in these cells that can be induced to fuse with the PM by insulin signaling.

Rab10 and Rab14 both associate with insulin-responsive GLUT4 vesicles

Given our ability to selectively visualize insulin-responsive GLUT4 vesicles with IRAP-pHluorin, we tested which Rab proteins were localized on these fusing vesicles. To monitor fusion, we tracked the intensities of candidate Rab proteins and IRAP-pHluorin at the fusion site by dual-color TIRF microscopy, quantifying events in which an IRAP-pHluorin signal coincided with the presence of a particular Rab-containing vesicle. To avoid counting a coincidental overlap of an IRAP fusion event with a Rab vesicle near the fusion site, we counted only Rab-associated IRAP-pHluorin fusion events in which there were similar intensity drops in both channels after fusion (see Materials and methods and Fig. S3).

stacks are generated with an interval of 1 frame; each individual fusion event is, therefore, represented by one bright spot in the projection. Bar, 4 µm. (B) The data are represented as mean ± SEM (error bars), *n* = 3 cells. (C–H) Adipocytes were cotransfected with IRAP-pHluorin and GLUT4-mCherry, and fusion events were analyzed using dual-color TIRF microscopy 3 min after insulin stimulation. (C) A full release event. Intensities measured from the fusion site and the adjacent annulus (see Materials and methods and Fig. S3) are plotted in E. IRAP and GLUT4 were completely released from the vesicle after fusion, with the fusion site intensities having already returned to the background level when the lateral diffusion stopped, as indicated by the annulus intensities dropping back to the background. Bar, 0.5 µm. (D) A partial release event. Intensities measured from the fusion site and the adjacent annulus are plotted in F. Only a small fraction of IRAP and GLUT4 were released from the vesicle during fusion; therefore, GLUT4 intensity of the vesicle was still above the background when annulus intensities of IRAP and GLUT4 returned to the baseline, which indicates closure of the fusion pore and attenuation of lateral diffusion. IRAP-pHluorin intensity of the vesicle had already dropped back to the background level at the time because of vesicular lumen reacidification while GLUT4-mCherry intensity persisted. Bar, 0.5 µm. (G) Summary of full versus partial releases of IRAP-pHluorin vesicles at the PM in adipocytes under insulin stimulation. Data are represented as mean ± SEM, *n* = 3 cells and 107 fusions. See also Video 1. (H) The presence of GLUT4-mCherry on insulin-stimulated IRAP-pHluorin fusing vesicles. Data are represented as mean ± SEM (error bars), *n* = 3 cells and 117 fusions.

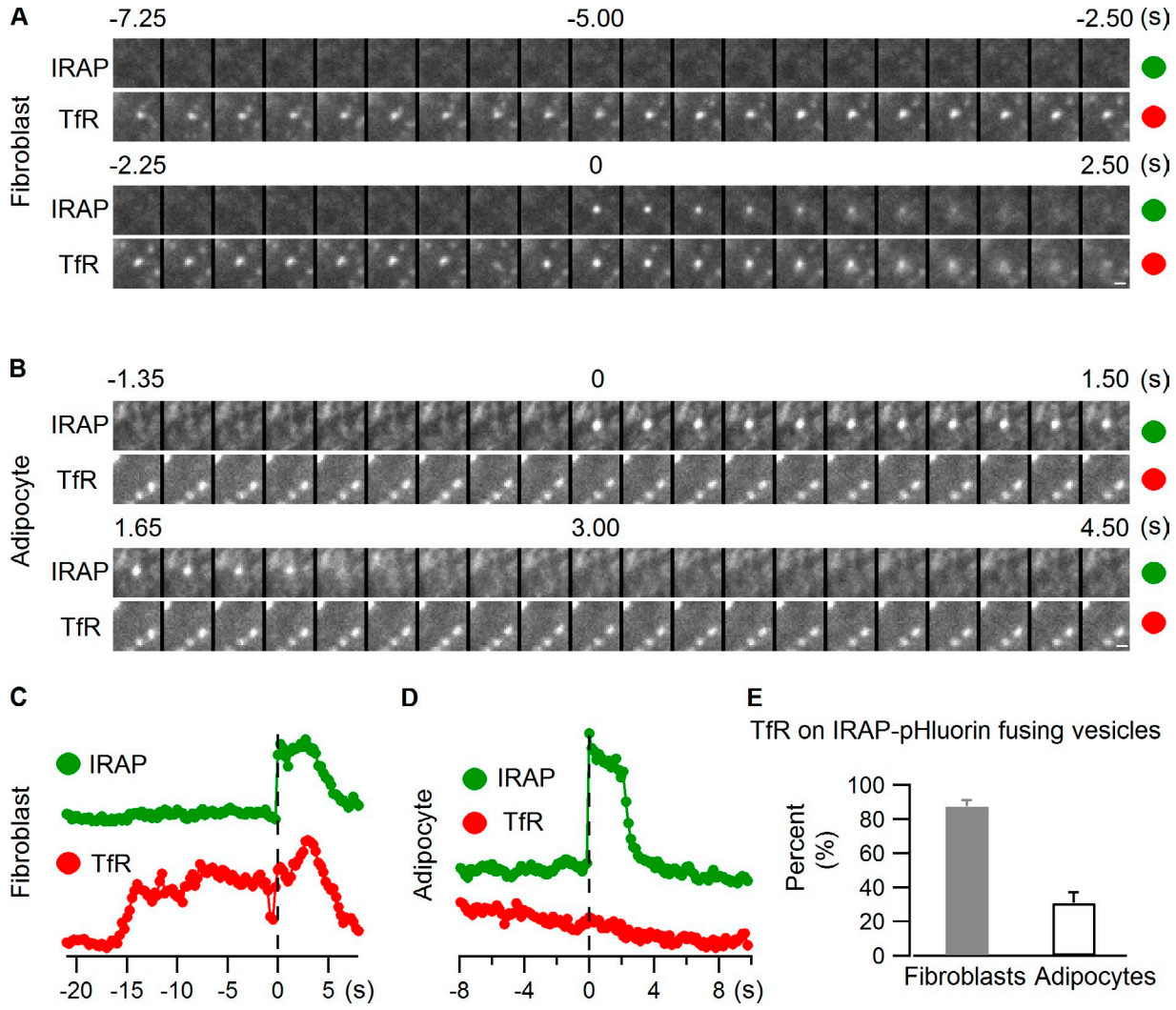

Figure 3. **Insulin mobilizes both GSVs and GLUT4-containing endosomal compartments.** IRAP-pHluorin and TfR-mCherry were cotransfected into 3T3-L1 fibroblast cells (A and C) and adipocytes (B and D), and IRAP-pHluorin fusion events were monitored using dual-color TIRF microscopy 3 min after insulin stimulation for the presence of TfR on the fusing vesicles. (A) An IRAP-pHluorin fusing vesicle with TfR associated with it observed in a 3T3-L1 fibroblast cell. Intensities within the fusion site were measured from both channels and plotted in C. Bar, 0.5 µm. (B) An IRAP-pHluorin fusion event without TfR association observed in an adipocyte. Intensities within the fusion site were measured from both channels and plotted in D. Bar, 0.5 µm. (E) Summary of the presence of TfR on insulin-stimulated IRAP-pHluorin fusing vesicles in 3T3-L1 fibroblasts and adipocytes. Data are represented as mean ± SEM (error bars). Fibroblasts, n = 3 cells and 28 fusions; adipocytes, n = 3 cells and 104 fusions. See also Fig. S2, and Videos 2 and 3.

Using this assay, we found that neither Rab4A nor Rab4B significantly resided on IRAP-pHluorin fusing vesicles elicited by insulin treatment (Fig. 4, A, E, and I; and Video 4). Because Rab4A and Rab4B showed overwhelming overlap with GLUT4 vesicles in the TIRF zone in nonstimulated cells, the early endosomes they reside on are likely very close to the PM and involved in GLUT4 recycling (Kaddai et al., 2009; Stenmark, 2009). Strikingly, Rab10 was found associated with most (>90%) of the IRAP-pHluorin fusing vesicles (Fig. 4, C, G, and I; and Video 5). Its low abundance on GLUT4 vesicles close to the PM in unstimulated cells (Fig. 1, A and B) suggests that the GLUT4 vesicles it labels only translocate to the PM in response to insulin. Rab14 exhibited moderate to low association with IRAP-pHluorin fusing vesicles (Fig. 4, D, H, and I; and Video 6), with the percentage being in the range of that seen for TfR in the IRAP-pHluorin assay. Other Rab proteins, including Rab8A (Fig. 4, B, F, and I; and Video 7), were occasionally seen on fusing vesicles, though at a much lower frequency than either Rab10 or Rab14 (Fig. 4 I).

Rab10 and Rab14 label distinct intracellular compartments

Because Rab10 and Rab14 both showed significant association with IRAP-pHluorin fusing vesicles in adipocytes, we further examined their intracellular distributions. Rab10 vesicles showed little overlap with Rab14 vesicles (Fig. 5, A and B), which suggests that each Rab protein was associated with a different intracellular compartment. Given that insulin stimulation in adipocytes mobilized both GSVs and GLUT4-containing endosomal compartments to deliver GLUT4 to the PM, the compartments labeled by Rab10 and Rab14 could correspond, respectively, to GSVs and endosomal compartments.

We tested this possibility by examining whether Rab10 or Rab14 vesicles near the PM colocalized with TfR. Rab10 vesicles had little TfR associated with them (Fig. 5, C and D), whereas Rab14 vesicles contained a remarkable amount of TfR (Fig. 5, E and F). The association of Rab14 with endosomal compartments carrying TfR and its extent of association with insulin-stimulated IRAP-pHluorin fusing vesicles fit nicely with our initial characterization of IRAP-pHluorin fusion events, in which ∼30% of the fusing vesicles were found to contain TfR (Fig. 3 E). Therefore, Rab10 is likely involved in insulin-stimulated translocation of GSVs to the PM, with Rab14 involved in insulin-stimulated translocation of GLUT4-containing endosomes.

Rab10 and Rab14 mediate insulin-stimulated GLUT4 translocation in parallel

To test the roles of Rab10 and Rab14 in GLUT4 translocation suggested by the IRAP-pHluorin assay, we knocked down Rab10 and Rab14 separately and together to see their effects on insulin-stimulated GLUT4 translocation (Fig. 6 A). Because Rab10 and/or Rab14 knockdown did not change GLUT4 distribution under basal conditions (Fig. 6 B), their observed effects are most likely through GLUT4 delivery to the PM. Knocking down Rab14 alone slightly reduced GLUT4 translocation to the PM, whereas Rab10 knockdown blocked GLUT4 translocation more severely. An additive inhibitory effect on insulin-stimulated GLUT4 translocation was observed when Rab10 and Rab14 were knocked down together (Fig. 6 C). Furthermore, putting back either Rab10 or Rab14 relieved part of the blockage on GLUT4 translocation caused by the loss of both of them (Fig. 6 D). Together, these data reveal that Rab10 and Rab14 function in GLUT4 translocation in parallel instead of sequentially. They further support the idea that Rab10 and Rab14 mediate insulin-stimulated GLUT4 translocation, respectively, of GSVs and endosomal compartments.

Insulin recruits Rab10-associated GSVs to the PM

Comparison of Rab10's behavior under insulin stimulation with that of other Rab proteins further supports Rab10's role in GSV mobilization. GFP-tagged Rab proteins together with GLUT4-mCherry were transfected into adipocytes, and their response to insulin stimulation was followed using dual-color TIRF microscopy. GFP-Rab10 responded to insulin stimulation by robustly and efficiently redistributing close to the PM in a coordinated manner with GLUT4-mCherry (Fig. 7, C, E, and F). None of the other Rabs (including Rab4A, Rab8A, and Rab14) exhibited this behavior, as no change in their distribution was observed in response to insulin, even though GLUT4 responded to insulin and redistributed to the PM in all cases (Fig. 7, A, B, and D). Few Rab10 vesicles were found close to the PM before insulin stimulation (Fig. 7 E). Shortly after insulin stimulation, however, Rab10 vesicles translocated to and docked at the PM (Fig. 7 F). Importantly, most Rab10 vesicles that were recruited to the TIRF zone contained GLUT4 (i.e., ∼50% of GLUT4 vesicles in the TIRF zone were Rab10 positive vs. <∼15% under basal conditions), which indicates that they were GLUT4 carriers and thus GSVs (Fig. 7 F).

Rab10 associates with intracellularly retained GSVs, trafficking in an AS160-dependent manner to the PM

To gain insight into the timing of Rab10 activation and its association with GLUT4 vesicles, we examined when Rab10 appears on GLUT4 vesicles as they are recruited to the PM under insulin signaling. As shown in Fig. 7 G for a representative event, Rab10 was already bound to GSVs when vesicles appeared in the TIRF zone and remained associated with GSVs as they moved close to the PM before fusion (all 27 vesicles from two cells that were analyzed showed this behavior). This suggested that Rab10 is activated and attaches to GLUT4 vesicles deep in the cell.

AS160 is proposed to inhibit GLUT4 translocation by inactivating Rab proteins needed for this translocation (Eguez et al., 2005; Larance et al., 2005). When AS160 is phosphorylated by Akt during insulin stimulation, its GAP activity is proposed to be inactivated (Sano et al., 2003). Rab proteins involved in GLUT4 dynamics thereby become active, resulting in GLUT4 redistribution to the PM (Sakamoto and Holman, 2008). To test whether Rab10 is downstream of AS160, we examined the effects of AS160 mutants on insulin recruitment of Rab10-marked GSVs. Notably, AS160-4P, the constitutively active form of AS160 (Sano et al., 2003), inhibited the movement of Rab10 vesicles to the PM by insulin (Fig. 8, A and C), whereas AS160-4P, R/A, which does not have a functional GAP domain (Sano et al., 2003), had no effect (Fig. 8, A and C). These data suggest Rab10 activation is regulated by AS160 GAP activity, and this activation is essential for Rab10 vesicles to be recruited close to the PM.

The functional status of Rab10 determines PM recruitment of GSVs

To further investigate Rab10's role in GSV mobilization to the PM in response to insulin in adipocytes, we coexpressed Rab10-QL, the constitutively active Rab10 mutant (Babbey et al., 2006; Sano et al., 2007), and GLUT4-mCherry in adipocytes. Before insulin stimulation, Rab10-QL–labeled vesicles enriched in GLUT4 were found docked at the PM, with more GLUT4 found constitutively at the PM (Fig. 8, B [0 min] and C). This suggests that activated Rab10 can trigger GSV translocation to the cell periphery, followed by PM docking and fusion independent of insulin or AS160 inactivation (Fig. S4). Upon insulin stimulation, the amount of GLUT4 delivered to the PM increased further (Fig. 8, B [6 min] and C), which indicates an additional effect of insulin on the fusion activity of Rab10-labeled GSVs. These findings indicate that PM recruitment of Rab10-labeled GSVs is controlled by the functional status of Rab10, which, in turn, is regulated by insulin through its effects on AS160 GAP activity. This supports previous work by Sano et al. (2007, 2008), who first suggested that Rab10 is an important component of the insulin signaling pathway regulating GLUT4 translocation.

Myosin-Va facilitates fusion of insulin-responsive GLUT4 vesicles at the PM

Rab proteins mediate vesicle trafficking by recruiting a variety of effectors (Hutagalung and Novick, 2011), and several classes

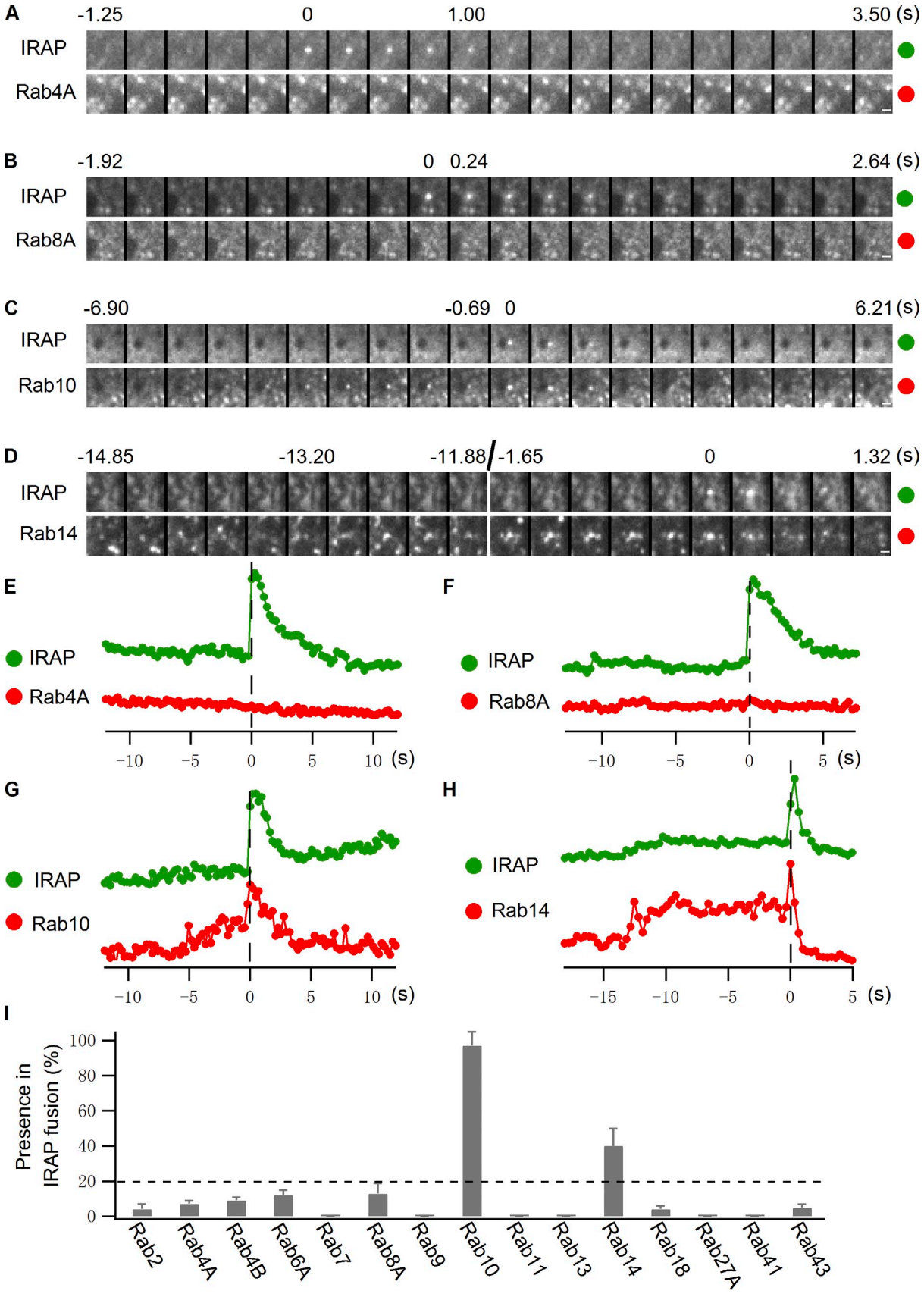

Figure 4. **Rab10 and Rab14 both associate with insulin-stimulated IRAP-pHluorin fusing vesicles.** (A–H) Rab4A, Rab8A, Rab10, and Rab14 tagged with TagRFP were separately transfected into adipocytes along with IRAP-pHluorin. IRAP-pHluorin fusion events were monitored using dual-color TIRF microscopy 3 min after insulin stimulation for the presence of a particular Rab protein on the fusing vesicles. (A and E) A Rab4A-negative IRAP-pHluorin fusion event. Fusion site intensities of both channels were measured from A and plotted in E. (B and F) A Rab8A-negative IRAP-pHluorin fusion event. Fusion site intensities

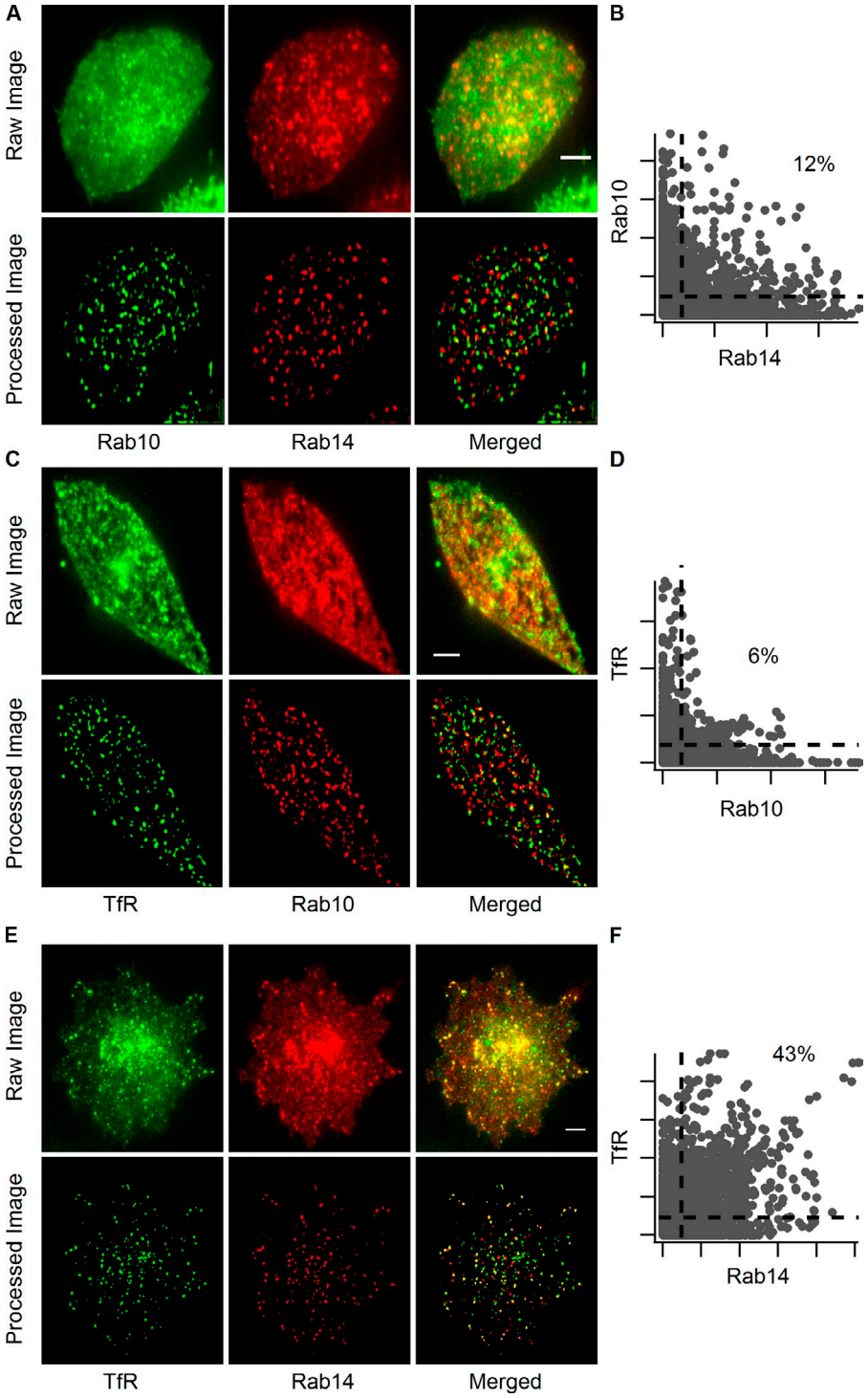

Figure 5. **Rab10 and Rab14 label distinct intracellular compartments.** Adipocytes were transfected with EGFP-Rab10 and TagRFP-Rab14 (A and B), TfR-EGFP and TagRFP-Rab10 (C and D), and TfR-EGFP and TagRFP-Rab14 (E and F), and their colocalization was examined using dual-color TIRF microscopy 3 min after insulin stimulation. Vesicles in the first rows (raw image) of A, C, and E were extracted and displayed in the second rows (processed image) to help visualize colocalization between vesicles (see Materials and methods and Fig. S3). Bars, 4 µm. Pixel intensity scatter plots (B, D, and F) of the processed images are to the right of the respective images. The dotted lines indicate 10% of the maximum intensities of different channels, and the percentages of pixels within the upper right regions are indicated.

of both channels are measured from B and plotted in F. (C and G) A Rab10-positive IRAP-pHluorin fusion event. Fusion site intensities of both channels are measured from C and plotted in G. (D and H) A Rab14-positive IRAP-pHluorin fusion event. Fusion site intensities of both channels are measured from D and plotted in H. Bars, 0.5 µm. (I) Summary of Rab protein associations with insulin-stimulated IRAP-pHluorin fusing vesicles. All Rab proteins were tagged with mKO, and their presence on insulin-stimulated IRAP-pHluorin fusing vesicles was quantified. The association of Rab4A, Rab8A, Rab10, and Rab14 with insulin-stimulated IRAP-pHluorin fusing vesicles was further tested with TagRFP-tagged Rabs. Switching fluorescent protein tags on the Rab proteins had no significant effect on the extent of association. Data are represented as mean ± SEM (error bars). The numbers of cells and insulin-stimulated IRAP-pHluorin fusing vesicles analyzed were as follows: Rab4A, 3 cells and 129 fusions; Rab8A, 3 cells and 136 fusions; Rab10, 3 cells and 143 fusions; and Rab14, 3 cells and 138 fusions. For each of the other Rab proteins, two cells were selected and >60 fusions were examined. The horizontal broken line indicates 20%, which is our threshold for significant association with IRAP-pHluorin fusing vesicles. See also Fig. S3 and Videos 4–7.

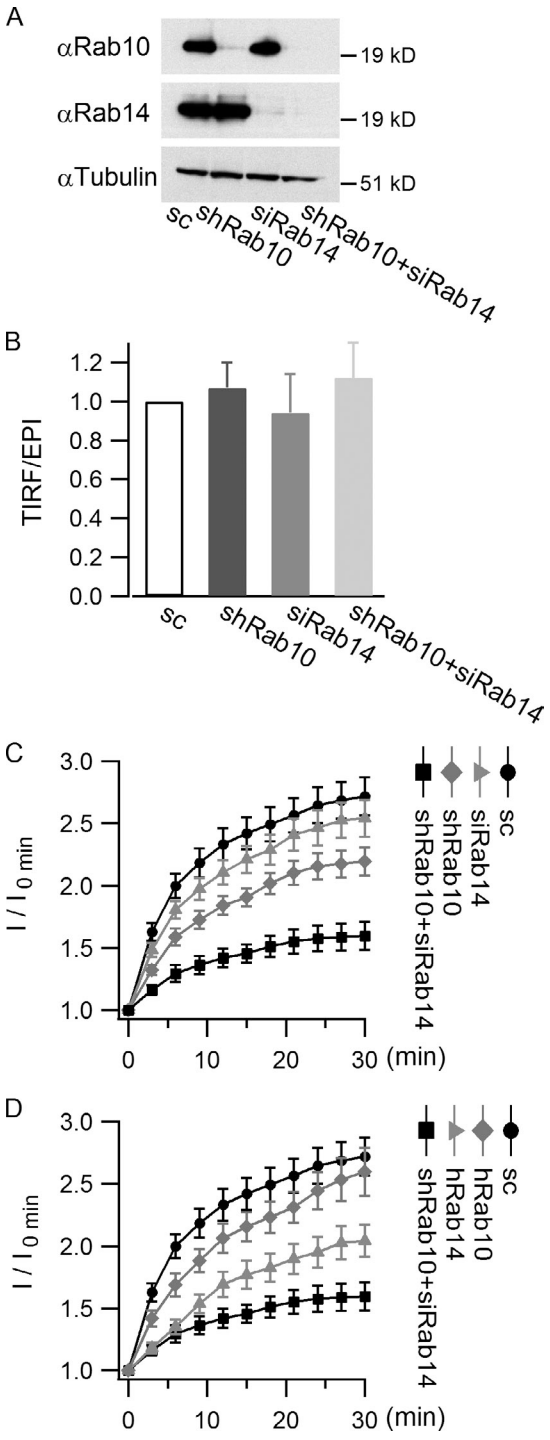

Figure 6. **Rab10 and Rab14 mediate GLUT4 translocation in parallel.** 3T3-L1 cells infected with HA-GLUT4-EGFP and scrambled shRNA or Rab10 shRNA were differentiated and then transfected with or without Rab14 siRNA. 48 h after transfection, insulin-stimulated GLUT4 translocation was measured using TIRF microscope. (A) Western blots showing knockdown efficiency of Rab10 and Rab14. (B) Loss of Rab10 and/or Rab14 does not change GLUT4 distribution under basal conditions. GLUT4 distribution under basal conditions was measured by the TIRF/epifluorescence (EPI) ratio, and the ratio was normalized to the control value. (C) The effects of loss of Rab10 and/or Rab14 on GLUT4 translocation. Insulin-stimulated GLUT4 translocation was indicated by TIRF image intensities (I) at different time points normalized to the intensity measured before insulin perfusion ($I_{0\ min}$). (D) Restoring Rab10 or Rab14 recovered part of GLUT4 translocation. TagRFP-Rab10 or TagRFP-Rab14 (both of human origin) was cotransfected with Rab14 siRNA into differentiated adipocytes, and GLUT4 translocation was measured 48 h after transfection. Data are represented as mean ± SEM (error bars). Scrambled, n = 37 cells; shRab10, n = 44 cells; siRab14, n = 31 cells; shRab10+siRab14, n = 33 cells; hRab10, n = 26 cells; hRab14, n = 29 cells.

of myosin motor proteins are known to function as Rab effectors to facilitate cargo transport (Seabra and Coudrier, 2004). Three myosin proteins, including myosin-1c (Bose et al., 2002), myosin II (Fulcher et al., 2008), and myosin-Va (Yoshizaki et al., 2007), have been implicated in GLUT4 translocation, although their specific roles in this process remain elusive. To investigate whether any of these myosin proteins localizes on GLUT4 vesicles, we examined their intracellular localization using dual-color TIRF microscopy. Myosin-1c distributed on the PM evenly, showing no vesicular labeling (Fig. 9 A). Myosin II localized to intracellular compartments, but exhibited no overlap with GLUT4 vesicles (Fig. 9 B). In contrast, the short-tail (ST) form of melanocyte myosin-Va (myosin-Va ST), which targets to membranes in an identical manner to the full-length melanocyte myosin-Va (Wu et al., 1998; Wu et al., 2002), displayed substantial overlap with GLUT4 vesicles (Fig. 9 C).

To further explore the association of myosin-Va with insulin-responsive GLUT4 vesicles, the IRAP-pHluorin fusion assay was performed. A large population of IRAP-pHluorin fusing vesicles had myosin-Va ST associated with them, whereas myosin-1c and myosin II were not seen on fusing vesicles (Fig. 9, D, E, and F; and Video 8). Myosin-Va ST colocalized with both Rab10 and Rab14 in adipocytes (Fig. 9, G and H) and could also be coprecipitated with Rab10 and Rab14 (Fig. S5). Therefore, myosin-Va directly associates with GSVs and GLUT4-containing endosomal compartments, and this association is likely formed through the interactions of myosin-Va with Rab10 and Rab14, respectively.

Myosin-Va ST lacks the actin-binding domain of the full-length myosin-Va. Therefore, at high expression levels, it can compete with endogenous myosin-Va to prevent the membrane structures it binds to from interacting with actin (Wu et al., 1998). We looked at the effect of overexpressing myosin-Va ST on IRAP-pHluorin translocation to the PM to assess the role of myosin-Va in GLUT4 translocation. High expression of myosin-Va ST in adipocytes substantially reduced insulin-stimulated IRAP-pHluorin translocation to the PM (Fig. 9, I and J), which indicates that engagement of endogenous myosin-Va by Rab10 on GSVs and Rab14 on GLUT4-containing endosomal compartments is essential for optimal GLUT4 delivery to the PM. When examined with GLUT4-EGFP in insulin-stimulated adipocytes, myosin-Va ST-associated GLUT4-EGFP vesicles were found to stay immobile at the cell periphery for extended times, and were incapable of fusing with the PM (Fig. 9 L). In contrast, insulin-responsive GLUT4-EGFP vesicles underwent efficient docking and fusion at the PM in control cells (Fig. 9 K). Myosin-Va, therefore, appears to be needed for ultimate fusion of insulin-responsive GLUT4 vesicles. Such a role is consistent with a recent study showing that the actin network beneath the PM is essential for GLUT4 vesicles fusion at the PM, but not for their recruitment to the cell periphery (Lopez et al., 2009).

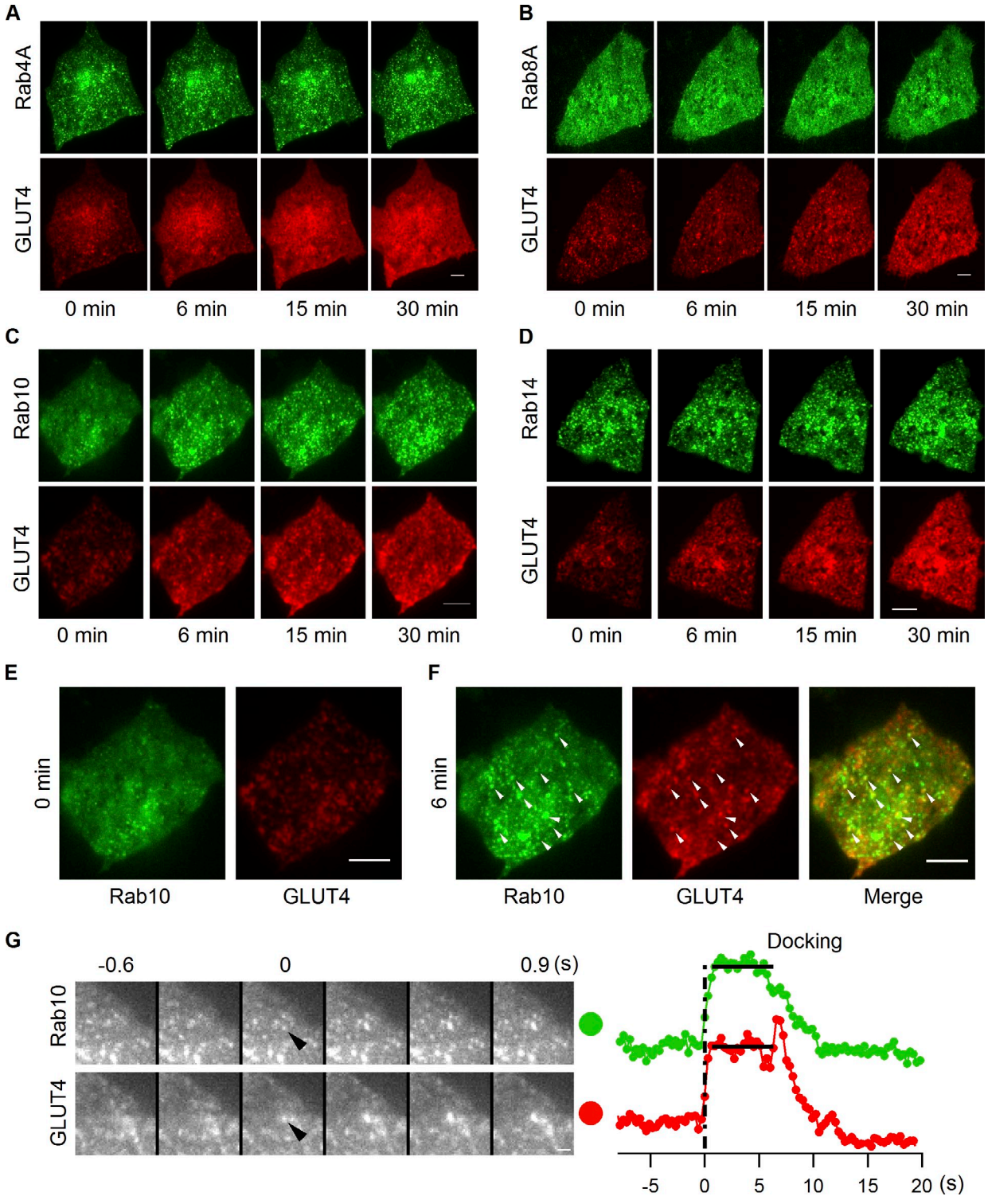

Figure 7. **Insulin recruits Rab10-marked GSVs to the PM.** EGFP-labeled Rab4A (A), Rab8A (B), Rab10 (C), and Rab14 (D) were separately transfected into adipocytes together with GLUT4-mCherry, and their insulin responsiveness was followed using dual-color TIRF microscopy. The first two columns in C are enlarged and displayed in E and F. Representative vesicles positive for both GLUT4 and Rab10 are indicated with arrowheads in F. Bars, 4 µm. (G) Rab10 gets activated and attaches to GSV before the vesicle gets into the TIRF zone. Adipocytes were cotransfected with EGFP-Rab10 and GLUT4-mCherry, and images were taken 3 min after insulin stimulation. Vesicle intensities measured from both channels are plotted on the right, and the docking stage is indicated with horizontal lines. Bars, 1 µm.

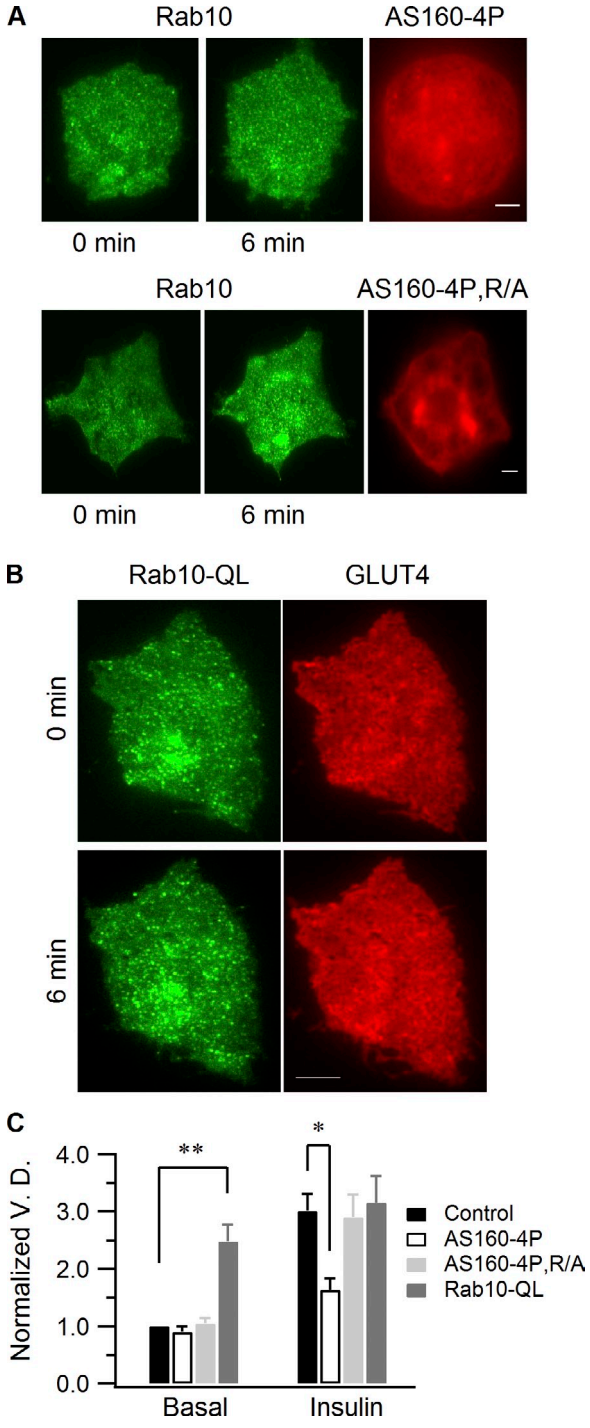

Figure 8. **AS160 regulates Rab10 recruitment by insulin stimulation.** (A) Adipocytes were transfected with EGFP-Rab10 and either mCherry-AS160-4P or mCherry-AS160-4P, R/A. Insulin-stimulated Rab10 vesicle recruitment to the cell periphery was followed using TIRF microscopy. AS160 images were taken using the epifluorescence mode. (B) EGFP-Rab10-QL and GLUT4-mCherry were transfected into adipocytes, and dual-color TIRF microscopy images were taken before and 6 min after insulin stimulation. Bars, 4 µm. (C) Rab10 vesicle density quantification. Rab10 vesicle densities were measured before and 6 min after insulin perfusion, and all densities were normalized to the mean of those measured from control cells before insulin stimulation. Data are represented as mean ± SEM (error bars). Control, $n = 9$ cells; AS160-4P, $n = 10$ cells; AS160-4P, R/A, $n = 9$ cells; Rab10-QL, $n = 12$ cells. **, $P < 0.02$; *, $P < 0.05$.

Discussion

GLUT4 follows a complex intracellular recycling itinerary that involves many steps. These include: GSV formation, release from intracellular retention, translocation to the PM, docking and fusion at the PM, endocytosis from the PM, and recycling in the endosomal system (Fig. 10 A). Rab proteins are important regulators of many of these steps, but what particular Rab protein controls which steps has been previously difficult to address. In this study, we used TIRF microscopy to monitor GLUT4 trafficking under basal conditions and during insulin signaling, seeking to identify Rab proteins associated with GSVs and their mode of action on GLUT4 trafficking. Screening a large set of Rab proteins for colocalization with GLUT4 for association with IRAP-pHluorin vesicles fusing at the PM in response to insulin stimulation, and for PM recruitment under insulin stimulation, we discovered that only Rab10 associates with GSVs and mediates GSV peripheral translocation after becoming activated. The Rab GTPase activation protein, AS160, negatively regulates Rab10 activity on GSVs, as constitutively active AS160 prevented Rab10-containing GVSs from translocating to the PM in response to insulin. Furthermore, we found that Rab10 interacts with the actin motor protein myosin-Va. This facilitates the translocation of GSVs to sites at the PM where they can fuse. Consistent with this, high expression levels of a short tail form of myosin-Va lacking the actin-binding domain decreased GLUT4 delivery to the PM.

These findings help clarify the insulin signaling transduction mechanism that regulates GLUT4 in the PM of adipocytes. They reveal an important role for Rab10 in GSV release from intracellular retention, recruitment to, and docking at the PM, and show that a myosin-Va–mediated step is needed for ultimate vesicle fusion. They also provide new insights into the GLUT4 trafficking defects observed upon knocking down Rab10 (Sano et al., 2007, 2008) and a Rab10-specific GEF DENND4C (Sano et al., 2011).

Besides revealing the role of Rab10 in GSV translocation to the PM, we also discovered that Rab14 mediates insulin-stimulated GLUT4 translocation to the PM via endosomal compartments, which contain both GLUT4 and TfR. Given that Rab14 is also a AS160 GAP domain substrate (Mîinea et al., 2005), this finding reveals an additional pathway for GLUT4 to reach the PM in response to insulin that is also regulated through AS160 (Fig. 10 A). The Rab14-mediated endosomal pathway functions in parallel with the Rab10-mediated GSV pathway to deliver GLUT4 to the PM in response to insulin. This endosomal pathway could help shift intracellular GLUT4 to the PM more efficiently under insulin stimulation as well as serve as a backup pathway to mobilize GLUT4 to the PM in the absence of Rab10. Such a role for Rab14 in GLUT4 trafficking is consistent with the findings that insulin stimulation increases TfR on the PM (Fig. S2 H), and that ablation of endosomes containing GLUT4 and TfR reduces insulin-stimulated GLUT4 translocation to the PM (Zeigerer et al., 2002).

We also found that Rab4a, Rab4b, and Rab8A colocalize with GLUT4, but do not associate with insulin-responsive GLUT4 compartments. Therefore, they likely participate in

recycling of GLUT4 through endosomal membranes after its delivery to the PM (Fig. 10 A). This would provide a mechanism to retrieve GLUT4 back to endosomal compartments and GSVs.

Our discovery that myosin-Va associates with insulin-responsive GLUT4 vesicles by interacting with Rab10 and Rab14 provides new molecular insights into how these vesicles navigate through the dense peripheral actin meshwork to position themselves for fusion with the PM in response to insulin. Previous studies have revealed a role for actin in efficient GLUT4 delivery to the PM (Omata et al., 2000; Kanzaki and Pessin, 2001; Lopez et al., 2009). Our work suggests how this may occur (Fig. 10 B). By engaging Rab10 on GSVs and Rab14 on GLUT4-containing endosomal compartments, myosin-Va could bridge individual insulin-responsive GLUT4 vesicles to the actin meshwork beneath the PM, directing them through the dense actin meshwork and then positioning them into the docking/fusion sites, where the ultimate fusion event occurs. Myosin-Va ST lacking the actin binding domain decouples insulin-responsive GLUT4 vesicles from the cortical actin network, leaving them at the ends of microtubules (Lizunov et al., 2005; Chen et al., 2008) and unable to access docking/fusion sites. Other myosin proteins, including myosin 1-C and myosin II, do not appear to be necessary for the final steps in GLUT4 delivery to the PM, although they could be important for earlier steps.

In summary, we provide live cell imaging data supporting the involvement of multiple Rab proteins in GLUT4 trafficking. Foremost is the critical role for Rab10 and myosin-Va in the regulation of GSV dynamics in adipocytes. In association with GSVs, GTP-bound Rab10 regulates GLUT4 levels in the PM by facilitating the GSV's translocation to and docking at the PM in response to insulin. These events are controlled upstream by insulin through tuning of AS160 GAP activity. Recruited GSVs with activated Rab10 then engage myosin-Va and other fusion factors to merge with the PM. In an alternative pathway, Rab14 mediates GLUT4 delivery to the PM via GLUT4-containing endosomal compartments, also in an insulin-responsive manner. This helps shift intracellular GLUT4 storage toward a greater buildup of GLUT4 on the PM. Myosin-Va serves as a common effector of Rab10 and Rab14, preparing insulin-responsive GLUT4 vesicles for fusion. Rab4A, Rab4B, and Rab8A may then recycle GLUT4 through the endosomal system after its delivery to the PM, retrieving GLUT4 back to GSVs and endosomal compartments, where Rab10 and Rab14 regulate their respective mobilization by insulin. Thus, multiple Rab proteins are important for ensuring a continuous supply of GLUT4 molecules to the PM for optimal insulin responsiveness.

Materials and methods

Cell culture and transfection

3T3-L1 fibroblast cells were grown in high-glucose DME supplemented with 10% newborn calf serum at 37°C and 5% CO_2. 2 d after reaching confluence, the fibroblast cells were incubated with the differentiation medium containing 10% FBS, 1 mM Rosiglitazone (Cayman Chemical), 1 mM bovine insulin, 0.5 mM 3-isobutyl-1-methylxanthine, and 0.25 mM dexamethasone for 3 d. Then the medium was changed to high-glucose DME containing 10% FBS and 1 mM bovine insulin for 2 d. Afterward, cells were maintained in DME with 10% FBS, and adipocytes typically became apparent beginning on the fourth day after addition of differentiation medium. 8–10 d after differentiation, 3T3-L1 adipocytes were treated with 0.25% trypsin-EDTA and pelleted. Adipocytes were resuspended in Cell Line Nucleofector Solution L (Lonza) and then transfected in cuvettes supplied with the transfection kit. For each gene, 4 µg of plasmid DNA was added into the solution. GLUT4 translocation and IRAP-pHluorin experiments were performed at 37°C 48 h after transfection. Insulin stimulation was applied at a final concentration of 100 nM. 3T3-L1 fibroblast cells infected with HA-GLUT4-EGFP (Muretta et al., 2008) and scrambled shRNA or siRab10 shRNA were provided by C.C. Mastick (University of Nevada, Reno, NV).

DNA constructs, siRNA knockdown, RT-PCR, and Western blotting

Rab1A, Rab2, Rab3A, Rab3B, Rab3D, Rab4A, Rab4B, Rab6A, Rab6B, Rab7, Rab8A, Rab8B, Rab9, Rab10, Rab11, Rab13, Rab14, Rab18, Rab21, Rab23, Rab26, Rab27A, Rab35, Rab41, and Rab43 of human origin were tagged at their N termini with mKO. EGFP- and TagRFP-tagged Rab4A, Rab4B, Rab8A, Rab10, and Rab14 were also constructed. Rab10-QL (Q68L) and Rab14-QL (Q70L) were tagged at the N terminus with FLAG. GLUT4-mCherry was made by tagging GLUT4 with mCherry at the C terminus. TfR were tagged with EGFP and mCherry at the C terminus. Myosin-1c, myosin II light chain and melanocyte myosin-Va short tail (MCST) were tagged with mCherry at their N termini. The fusion protein generated by melanocyte myosin-Va short tail construct contains the C-terminal 619 amino acids of the predominant spliced isoform found in melanocytes (including both melanocyte-specific exons, exon D and exon F, but not exon B; Seperack et al., 1995). Melanocyte myosin-Va long tail (MCLT) encodes the C-terminal 786 amino acids of melanocyte-specific myosin-Va (including exons D and F but not B). The predominant spliced isoform of myosin-Va found in brain (BRLT) contains exon B but not exon D or F. MC (−D) and MC (−F) LTs were generated by, respectively, deleting exons D and F from MCLT. Myosin-Va with different combination of exons were tagged with EGFP at their N termini (Wu et al., 2002). RT-PCR primers were designed as follows: 5′-AATACAATGACAGATTCCACAATT-3′ and 5′-TCAGTTGTTTCTTCAGTTTC-3′, spanning from exon C to after exon F (Seperack et al., 1995), to probe the splicing variants of myosin-Va in 3T3-L1 fibroblasts and adipocytes. Western blotting was performed as described previously, and DIL-2 was used to detect endogenous myosin-Va (Wu et al., 1997, 2002). Antibody DIL-2 was raised in rabbit against a GST fusion protein containing myosin V heavy chain residues 910–1,106, which correspond to the first segment of a helical coiled-coil in the central rod domain and were applied a in Western blot with a dilution of 1:4,000. GLUT4 (ab654, rabbit polyclone, 1:1,000), Rab10 (D36C4, rabbit monoclone, 1:2,000), Akt (C67E7, rabbit monoclone, 1:3,000), pAkt (Ser473; D9E, rabbit polyclone, 1:2,000), and Rab14 (R0781, rabbit polyclone, 1:1,000) antibodies were purchased from Abcam, Cell Signaling Technology, and Sigma-Aldrich, respectively. SMARTpool siRNA against Rab14 and the scrambled control were purchased from Thermo Fisher Scientific, Inc. Rab14 target sequences are as follow: 5′-ACGCAAGGAAUCUCACCAA-3′, 5′-ACAUAUAACCACUUAAGCA-3′, 5′-CAGGUGCGCUCAUGGUGUA-3′, and 5′-GGUGUUGAAUUUGGUACAA-3′. The Rab10 target sequence is 5′-GCATCATGCTAGTGTATGA-3′.

TIRF microscopy, data process, and quantification

TIRF microscopy images were acquired using a True MultiColor Laser TIRFM system (Leica) equipped with a high-speed EM charge-coupled device camera (C9100-13; Hamamatsu Photonics), a HCX Plan-Apochromat 100× objective lens (NA 1.46; Leica), a C-mount 1.6× expansion lens, and Leica AF6000 software. During imaging, cells were kept in phenol red–free DME (Invitrogen) at 37°C. Two-color acquisition was achieved by fast switching excitation lasers so that images from green and red channels were aligned perfectly. To capture IRAP-pHluorin fusion events, adipocytes showing no vesicle fusion before insulin stimulation were preferentially chosen because they usually responded to insulin very well, producing many fusion events after stimulation.

ImageJ and custom-written Matlab programs were used to process images. To quantify colocalization between GLUT4 and Rab proteins (Fig. 1), 2–3 cells were selected for a particular Rab protein, and in each cell GLUT4 vesicles in a selected region were examined for the presence of the Rab protein. In Fig. S2, all vesicles in a particular region were categorized into GLUT4 only, GLUT4 & TfR, and TfR only based on the presence of GLUT4 and TfR on the vesicle. Measurements of the intensities from the fusion site and the adjacent annulus are illustrated in Fig. S3 B and have also been described previously (Bai et al., 2007).

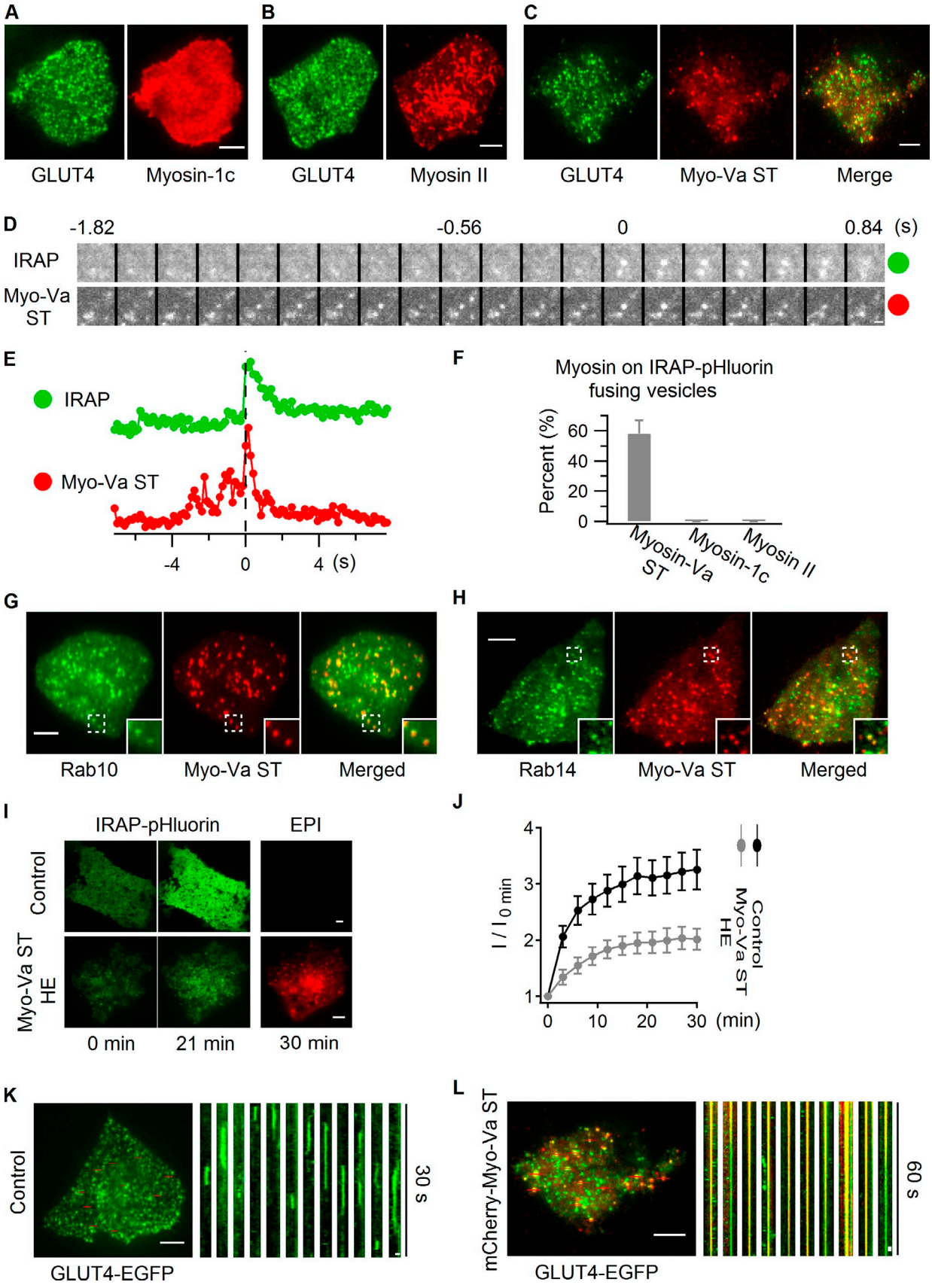

Figure 9. **Myosin-Va prepares insulin-responsive GLUT4 vesicles for fusion.** (A–C) Myosin-1c (A), myosin II (B), and myosin-Va short tail (ST; C) tagged with mCherry were separately transfected into adipocytes together with GLUT4-EGFP, and their colocalization was examined using dual-color TIRF microscopy. Images displayed were taken before insulin stimulation. (D–F) mCherry-tagged myosin-1c, myosin II, and myosin-Va ST were separately transfected

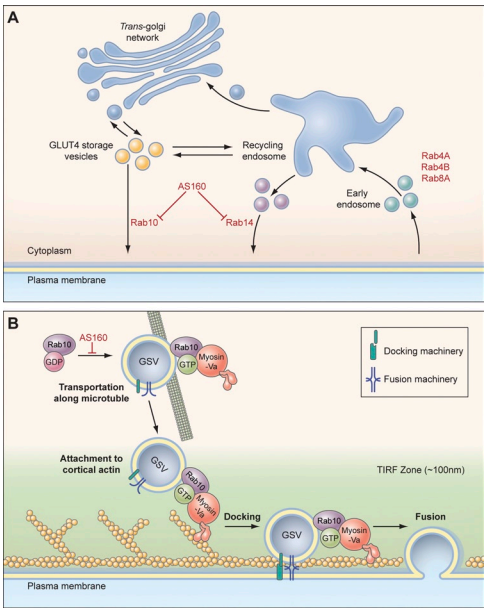

Figure 10. **Schematic models of GLUT4 trafficking in adipocytes.** (A) In response to insulin stimulation, Rab10 mediates GLUT4 translocation to the PM via GSVs, and Rab14 does so via TfR-positive endosomal compartments. Rab4A, Rab4B, and Rab8A mediate GLUT4 recycling after endocytosis. (B) After being activated inside the cell, Rab10 attaches to GSVs, recruits myosin-Va, and releases the intracellular retention of the vesicles. GSVs then move along microtubules close to the PM. In the periphery, GSVs transition to actin filaments beneath the PM and use myosin-Va to get into sites on the PM, where docking and fusion machineries are located.

To determine the percentage of Rab-positive and -negative fusion, 2–3 cells were analyzed for each Rab protein. For each cell, a dual-color TIRF microscopy video of 200 frames with an exposure time (covering a two-channel cycle) around 200 ms was acquired 3 min after insulin stimulation. Normally, ~30–50 fusion events were easily identified in a video. Categorization of fusion events is quite straightforward in most cases. In a few cases, where local Rab vesicle density was high, there were chances that a fusion event could coincidently overlap with one Rab vesicle near the fusion site. When residing on the IRAP-pHluorin fusing vesicle, Rab10 and Rab14 diffused away along with IRAP-pHluorin after fusion, as did GLUT4 and TfR (Fig. 2, E and F; and Fig. 3 C), resulting in similar intensity drops in green and red channels (Fig. 4, G and H). However, in cases where coincidental overlap occurred, a similar intensity drop was not observed (Fig. S3). So the classification criteria used here specified that a Rab-associated IRAP-pHluorin fusion be counted only if there were similar intensity drops observed in both channels. The same rule also applied to classification of TfR and myosin proteins association with IRAP-pHluorin fusion events.

To measure the intensity ratio of the TIRF image to the epifluorescence one, the laser intensity was kept constant for each individual cell, and only the penetration depth was adjusted. The penetration depth of 90 nm was used for TIRF imaging, and the laser was straightened up to acquire the epifluorescence image. All ratios were normalized to the mean value of the control cells. To monitor and quantify insulin-stimulated GLUT4-EGFP and IRAP-pHluorin translocation to the PM, TIRF images were first taken under basal conditions, and image intensities were measured ($I_{0\ min}$). Insulin was then perfused, and TIRF images were taken over 30 min with an interval of 3 min. Intensities measured over time (I) are normalized with $I_{0\ min}$ ($I/I_{0\ min}$) and plotted against the time to indicate the time course of GLUT4-EGFP and IRAP-pHluorin translocation to the PM.

To remove diffusive uneven background, enhance vesicular feature, and quantify the number of vesicles, raw images were processed as described in the legend for Fig. S3.

Statistical analysis

Data are presented as means ± SEM unless otherwise indicated. A Student's *t* test (unpaired, two-tailed) was used in GraphPad Prism 5 (GraphPad Software).

Online supplemental material

Fig. S1 shows several examples of Rab proteins not overlapping with GLUT4. Fig. S2 compares the localization of GLUT4 and TfR in 3T3-L1 fibroblast cells and adipocytes. Fig. S3 shows an IRAP-pHluorin vesicle fusing close to a Rab4A vesicle and illustrates the algorithms applied in this study to quantify vesicle numbers. Fig. S4 shows the effects of Rab10QL expression on the insulin signaling pathway and GLUT4 distribution. Fig. S5 shows the interaction of myosin-Va with Rab10 and Rab14. Video 2 shows the presence of TfR in IRAP-pHluorin fusions in 3T3-L1 fibroblast cells. Videos 1 and 3–8 show the presence of GLUT4, TfR, Rab4A, Rab10, Rab14, Rab8A, and myosin-Va ST in IRAP-pHluorin fusions in 3T3-L1 adipocytes. Table S1 summaries the localization of all candidate Rab proteins. Online supplemental material is available at http://www.jcb.org/cgi/content/full/jcb.201111091/DC1.

We thank Dr. Marci Scidmore, Dr. Michael D. Ehlers, and Dr. Gustav E. Lienhard for sharing reagents; Dr. Cynthia C. Mastick for providing 3T3-L1 cells infected with HA-GLUT4-EGFP and scrambled or siRab10 shRNA; Dr. Owen Schwartz, Dr. Lily Koo, and Dr. Steven Becker for assistance with microscopy; and members of Tao Xu's and Jennifer Lippincott-Schwartz's groups for valuable advice.

This work was supported by grants from the Major State Basic Research Program of the People's Republic of China (2010CB833701), the National Science Foundation of China (30900268), and the Beijing Natural Science Foundation (5092017).

Submitted: 21 November 2011
Accepted: 13 July 2012

References

Babbey, C.M., N. Ahktar, E. Wang, C.C. Chen, B.D. Grant, and K.W. Dunn. 2006. Rab10 regulates membrane transport through early endosomes of polarized Madin-Darby canine kidney cells. *Mol. Biol. Cell.* 17:3156–3175. http://dx.doi.org/10.1091/mbc.E05-08-0799

Bai, L., Y. Wang, J. Fan, Y. Chen, W. Ji, A. Qu, P. Xu, D.E. James, and T. Xu. 2007. Dissecting multiple steps of GLUT4 trafficking and

into adipocytes together with IRAP-pHluorin. The association of these myosin proteins with IRAP-pHluorin fusing vesicles was monitored using dual-color TIRF microscopy 3 min after insulin stimulation. (D) An IRAP-pHluorin fusing vesicle with myosin-Va ST associated with it. Fusion site intensities are measured from both channels and plotted in E. Also see Video 8. (F) Summary of myosin proteins' association with insulin-stimulated IRAP-pHluorin fusing vesicles. Data are represented as mean ± SEM (error bars). Myosin-Va ST, $n = 3$ cells and 122 fusions; for either of myosin-1c and myosin II, 2 cells and >60 fusions were examined. To capture a sufficient number of fusion events when myosin-Va ST was expressed, cells with low expression levels of myosin-Va ST were specifically chosen. (G and H) EGFP-Rab10 and EGFP-Rab14 were separately transfected into adipocytes together with mCherry-myosin-Va ST, and their overlap was examined using dual-color TIRF microscopy 3 min after insulin stimulation. Inset panels show enlarged views of the boxed regions. See also Fig. S5. (I and J) IRAP-pHluorin was transfected alone (Control) or with mCherry-myosin-Va ST into adipocytes, and insulin-stimulated IRAP-pHluorin translocation was followed using TIRF microscopy. Insulin-stimulated IRAP translocation was indicated by TIRF image intensities (I) at different time points normalized to the intensity measured before insulin perfusion ($I_{0\ min}$). Images of myosin-Va ST were taken using the epifluorescence mode. To obtain the optimal inhibitory effect, cells with myosin-Va ST expressed at high levels were specifically chosen (HE, high expression). In J, data are represented as mean ± SEM (error bars). Control, $n = 11$ cells; Myo-Va ST HE, $n = 14$ cells. (K and L) GLUT4-EGFP was transfected alone (K) or with mCherry-myosin-Va ST (L) into adipocytes. TIRF microscopy images taken 3 min after insulin stimulation are displayed on the left. The effects of myosin-Va ST association on GLUT4 vesicle dynamics are presented using kymographs on the right. Cells with myosin-Va ST expressed at high levels were specifically chosen for the myosin-Va ST group. Bars: (A–C) 4 µm; (D) 0.5 µm; (G, H, and I) 4 µm; (K and L, left) 4 µm; (K and L, right) 0.5 µm.

identifying the sites of insulin action. *Cell Metab.* 5:47–57. http://dx.doi.org/10.1016/j.cmet.2006.11.013

Bose, A., A. Guilherme, S.I. Robida, S.M. Nicoloro, Q.L. Zhou, Z.Y. Jiang, D.P. Pomerleau, and M.P. Czech. 2002. Glucose transporter recycling in response to insulin is facilitated by myosin Myo1c. *Nature*. 420:821–824. http://dx.doi.org/10.1038/nature01246

Bryant, N.J., R. Govers, and D.E. James. 2002. Regulated transport of the glucose transporter GLUT4. *Nat. Rev. Mol. Cell Biol.* 3:267–277. http://dx.doi.org/10.1038/nrm782

Chen, Y., Y. Wang, W. Ji, P. Xu, and T. Xu. 2008. A pre-docking role for microtubules in insulin-stimulated glucose transporter 4 translocation. *FEBS J.* 275:705–712. http://dx.doi.org/10.1111/j.1742-4658.2007.06232.x

Cormont, M., J.F. Tanti, A. Zahraoui, E. Van Obberghen, A. Tavitian, and Y. Le Marchand-Brustel. 1993. Insulin and okadaic acid induce Rab4 redistribution in adipocytes. *J. Biol. Chem.* 268:19491–19497.

Eguez, L., A. Lee, J.A. Chavez, C.P. Miinea, S. Kane, G.E. Lienhard, and T.E. McGraw. 2005. Full intracellular retention of GLUT4 requires AS160 Rab GTPase activating protein. *Cell Metab.* 2:263–272. http://dx.doi.org/10.1016/j.cmet.2005.09.005

Foley, K., S. Boguslavsky, and A. Klip. 2011. Endocytosis, recycling, and regulated exocytosis of glucose transporter 4. *Biochemistry*. 50:3048–3061. http://dx.doi.org/10.1021/bi2000356

Fulcher, F.K., B.T. Smith, M. Russ, and Y.M. Patel. 2008. Dual role for myosin II in GLUT4-mediated glucose uptake in 3T3-L1 adipocytes. *Exp. Cell Res.* 314:3264–3274. http://dx.doi.org/10.1016/j.yexcr.2008.08.007

Huang, S., L.M. Lifshitz, C. Jones, K.D. Bellve, C. Standley, S. Fonseca, S. Corvera, K.E. Fogarty, and M.P. Czech. 2007. Insulin stimulates membrane fusion and GLUT4 accumulation in clathrin coats on adipocyte plasma membranes. *Mol. Cell. Biol.* 27:3456–3469. http://dx.doi.org/10.1128/MCB.01719-06

Hutagalung, A.H., and P.J. Novick. 2011. Role of Rab GTPases in membrane traffic and cell physiology. *Physiol. Rev.* 91:119–149. http://dx.doi.org/10.1152/physrev.00059.2009

Jiang, L., J. Fan, L. Bai, Y. Wang, Y. Chen, L. Yang, L. Chen, and T. Xu. 2008. Direct quantification of fusion rate reveals a distal role for AS160 in insulin-stimulated fusion of GLUT4 storage vesicles. *J. Biol. Chem.* 283:8508–8516. http://dx.doi.org/10.1074/jbc.M708688200

Kaddai, V., T. Gonzalez, F. Keslair, T. Grémeaux, S. Bonnafous, J. Gugenheim, A. Tran, P. Gual, Y. Le Marchand-Brustel, and M. Cormont. 2009. Rab4b is a small GTPase involved in the control of the glucose transporter GLUT4 localization in adipocyte. *PLoS ONE*. 4:e5257. http://dx.doi.org/10.1371/journal.pone.0005257

Kandror, K.V., and P.F. Pilch. 1994. gp160, a tissue-specific marker for insulin-activated glucose transport. *Proc. Natl. Acad. Sci. USA*. 91:8017–8021. http://dx.doi.org/10.1073/pnas.91.17.8017

Kane, S., H. Sano, S.C. Liu, J.M. Asara, W.S. Lane, C.C. Garner, and G.E. Lienhard. 2002. A method to identify serine kinase substrates. Akt phosphorylates a novel adipocyte protein with a Rab GTPase-activating protein (GAP) domain. *J. Biol. Chem.* 277:22115–22118. http://dx.doi.org/10.1074/jbc.C200198200

Kanzaki, M., and J.E. Pessin. 2001. Insulin-stimulated GLUT4 translocation in adipocytes is dependent upon cortical actin remodeling. *J. Biol. Chem.* 276:42436–42444. http://dx.doi.org/10.1074/jbc.M108297200

Larance, M., G. Ramm, J. Stöckli, E.M. van Dam, S. Winata, V. Wasinger, F. Simpson, M. Graham, J.R. Junutula, M. Guilhaus, and D.E. James. 2005. Characterization of the role of the Rab GTPase-activating protein AS160 in insulin-regulated GLUT4 trafficking. *J. Biol. Chem.* 280:37803–37813. http://dx.doi.org/10.1074/jbc.M503897200

Lizunov, V.A., H. Matsumoto, J. Zimmerberg, S.W. Cushman, and V.A. Frolov. 2005. Insulin stimulates the halting, tethering, and fusion of mobile GLUT4 vesicles in rat adipose cells. *J. Cell Biol.* 169:481–489. http://dx.doi.org/10.1083/jcb.200412069

Lopez, J.A., J.G. Burchfield, D.H. Blair, K. Mele, Y. Ng, P. Vallotton, D.E. James, and W.E. Hughes. 2009. Identification of a distal GLUT4 trafficking event controlled by actin polymerization. *Mol. Biol. Cell*. 20:3918–3929. http://dx.doi.org/10.1091/mbc.E09-03-0187

Maxfield, F.R., and T.E. McGraw. 2004. Endocytic recycling. *Nat. Rev. Mol. Cell Biol.* 5:121–132. http://dx.doi.org/10.1038/nrm1315

Miesenböck, G., D.A. De Angelis, and J.E. Rothman. 1998. Visualizing secretion and synaptic transmission with pH-sensitive green fluorescent proteins. *Nature*. 394:192–195. http://dx.doi.org/10.1038/28190

Mîinea, C.P., H. Sano, S. Kane, E. Sano, M. Fukuda, J. Peränen, W.S. Lane, and G.E. Lienhard. 2005. AS160, the Akt substrate regulating GLUT4 translocation, has a functional Rab GTPase-activating protein domain. *Biochem. J.* 391:87–93. http://dx.doi.org/10.1042/BJ20050887

Muretta, J.M., I. Romenskaia, and C.C. Mastick. 2008. Insulin releases Glut4 from static storage compartments into cycling endosomes and increases the rate constant for Glut4 exocytosis. *J. Biol. Chem.* 283:311–323. http://dx.doi.org/10.1074/jbc.M705756200

Omata, W., H. Shibata, L. Li, K. Takata, and I. Kojima. 2000. Actin filaments play a critical role in insulin-induced exocytotic recruitment but not in endocytosis of GLUT4 in isolated rat adipocytes. *Biochem. J.* 346:321–328. http://dx.doi.org/10.1042/0264-6021:3460321

Ross, S.A., H.M. Scott, N.J. Morris, W.Y. Leung, F. Mao, G.E. Lienhard, and S.R. Keller. 1996. Characterization of the insulin-regulated membrane aminopeptidase in 3T3-L1 adipocytes. *J. Biol. Chem.* 271:3328–3332. http://dx.doi.org/10.1074/jbc.271.6.3328

Sakamoto, K., and G.D. Holman. 2008. Emerging role for AS160/TBC1D4 and TBC1D1 in the regulation of GLUT4 traffic. *Am. J. Physiol. Endocrinol. Metab.* 295:E29–E37. http://dx.doi.org/10.1152/ajpendo.90331.2008

Sano, H., S. Kane, E. Sano, C.P. Mîinea, J.M. Asara, W.S. Lane, C.W. Garner, and G.E. Lienhard. 2003. Insulin-stimulated phosphorylation of a Rab GTPase-activating protein regulates GLUT4 translocation. *J. Biol. Chem.* 278:14599–14602. http://dx.doi.org/10.1074/jbc.C300063200

Sano, H., L. Eguez, M.N. Teruel, M. Fukuda, T.D. Chuang, J.A. Chavez, G.E. Lienhard, and T.E. McGraw. 2007. Rab10, a target of the AS160 Rab GAP, is required for insulin-stimulated translocation of GLUT4 to the adipocyte plasma membrane. *Cell Metab.* 5:293–303. http://dx.doi.org/10.1016/j.cmet.2007.03.001

Sano, H., W.G. Roach, G.R. Peck, M. Fukuda, and G.E. Lienhard. 2008. Rab10 in insulin-stimulated GLUT4 translocation. *Biochem. J.* 411:89–95. http://dx.doi.org/10.1042/BJ20071318

Sano, H., G.R. Peck, A.N. Kettenbach, S.A. Gerber, and G.E. Lienhard. 2011. Insulin-stimulated GLUT4 protein translocation in adipocytes requires the Rab10 guanine nucleotide exchange factor Dennd4C. *J. Biol. Chem.* 286:16541–16545. http://dx.doi.org/10.1074/jbc.C111.228908

Schwartz, S.L., C. Cao, O. Pylypenko, A. Rak, and A. Wandinger-Ness. 2007. Rab GTPases at a glance. *J. Cell Sci.* 120:3905–3910. http://dx.doi.org/10.1242/jcs.015909

Seabra, M.C., and E. Coudrier. 2004. Rab GTPases and myosin motors in organelle motility. *Traffic*. 5:393–399. http://dx.doi.org/10.1111/j.1398-9219.2004.00190.x

Seperack, P.K., J.A. Mercer, M.C. Strobel, N.G. Copeland, and N.A. Jenkins. 1995. Retroviral sequences located within an intron of the dilute gene alter dilute expression in a tissue-specific manner. *EMBO J.* 14:2326–2332.

Stenmark, H. 2009. Rab GTPases as coordinators of vesicle traffic. *Nat. Rev. Mol. Cell Biol.* 10:513–525. http://dx.doi.org/10.1038/nrm2728

Sun, Y., P.J. Bilan, Z. Liu, and A. Klip. 2010. Rab8A and Rab13 are activated by insulin and regulate GLUT4 translocation in muscle cells. *Proc. Natl. Acad. Sci. USA*. 107:19909–19914. http://dx.doi.org/10.1073/pnas.1009523107

Watson, R.T., M. Kanzaki, and J.E. Pessin. 2004. Regulated membrane trafficking of the insulin-responsive glucose transporter 4 in adipocytes. *Endocr. Rev.* 25:177–204. http://dx.doi.org/10.1210/er.2003-0011

Wu, X., B. Bowers, Q. Wei, B. Kocher, and J.A. Hammer III. 1997. Myosin V associates with melanosomes in mouse melanocytes: evidence that myosin V is an organelle motor. *J. Cell Sci.* 110:847–859.

Wu, X., B. Bowers, K. Rao, Q. Wei, and Hammer JA III. 1998. Visualization of melanosome dynamics within wild-type and dilute melanocytes suggests a paradigm for myosin V function In vivo. *J. Cell Biol.* 143:1899–1918. http://dx.doi.org/10.1083/jcb.143.7.1899

Wu, X., F. Wang, K. Rao, J.R. Sellers, and J.A. Hammer III. 2002. Rab27a is an essential component of melanosome receptor for myosin Va. *Mol. Biol. Cell*. 13:1735–1749. http://dx.doi.org/10.1091/mbc.01-12-0595

Xu, Y., B.R. Rubin, C.M. Orme, A. Karpikov, C. Yu, J.S. Bogan, and D.K. Toomre. 2011. Dual-mode of insulin action controls GLUT4 vesicle exocytosis. *J. Cell Biol.* 193:643–653. http://dx.doi.org/10.1083/jcb.201008135

Yoshizaki, T., T. Imamura, J.L. Babendure, J.C. Lu, N. Sonoda, and J.M. Olefsky. 2007. Myosin 5a is an insulin-stimulated Akt2 (protein kinase Bbeta) substrate modulating GLUT4 vesicle translocation. *Mol. Cell. Biol.* 27:5172–5183. http://dx.doi.org/10.1128/MCB.02298-06

Zeigerer, A., M.A. Lampson, O. Karylowski, D.D. Sabatini, M. Adesnik, M. Ren, and T.E. McGraw. 2002. GLUT4 retention in adipocytes requires two intracellular insulin-regulated transport steps. *Mol. Biol. Cell*. 13:2421–2435. http://dx.doi.org/10.1091/mbc.E02-02-0071